ELSEVIER

Biochimica et Biophysica Acta 1313 (1996) 277–282

BBA Biochimica et Biophysica Acta

The crystal structure of annexin VI indicates relative rotation of the two lobes upon membrane binding

Hiroshi Kawasaki [a,c], Agustin Avila-Sakar [a,b], Carl E. Creutz [b], Robert H. Kretsinger [a,*]

[a] *Department of Biology, University of Virginia, Charlottesville, VA 22903, USA*
[b] *Department of Pharmacology, University of Virginia, Charlottesville, VA 22908, USA*
[c] *Department of Molecular Biology, Tokyo Metropolitan Institute of Medical Science, 3-18-22, Honkomagome, Bunkyo-ku, Tokyo 113, Japan*

Received 17 June 1996; accepted 19 June 1996

Abstract

The crystal structure of bovine liver annexin VI has been determined to low resolution by molecular replacement. The first lobe (domains 1–4) is rotated about 90° relative to the second lobe (domains 5–8). Since the same crystal form ($P4_3$, $68 \times 68 \times 205$ Å) grew from $(NH_4)_2SO_4$, polyethylene glycol, and sodium acetate with and without added calcium, this probably reflects the structure in solution. When bound to a lipid monolayer both lobes of annexin VI are coplanar. This implies a significant change in conformation upon binding to membranes.

Keywords: Annexin VI; Membrane binding; Calcium; Conformational change; Crystallography; Molecular replacement; (Bovine liver)

1. Introduction

Annexin VI is unique because it has eight domains. All other annexins have four domains, each of which is about 69 amino acids long and has five α-helices. Each domain has two interhelix loops on the inferred membrane binding surface that may coordinate calcium jointly with phospholipid headgroups. This calcium-dependent binding to phospholipids and membrane surfaces is one of the defining characteristics of annexins.

The four domains pack together to form a trapezoidal lobe about 60 by 40 Å in surface area. The lobe is about 30 Å thick and has an approximate two fold axis of rotation perpendicular to the membrane surface, as seen in the crystal structures of annexin V [1], annexin I [2], annexin IV [3], and annexin III [4]. This local two fold axis relates domains 1 and 2 to domains 3 and 4. By homology [5] domains 5 and 6 of annexin VI are inferred to be related to domains 7 and 8.

We saw peanut-shaped projected densities in images reconstructed from electron micrographs of microcrystals of annexin VI [6]; however, we could not resolve individual molecules nor infer the orientations of the two lobes. Electron micrographs of annexin VI bound to phospholipid monolayers were interpreted [7] as indicating that both lobes are coplanar. However, the resolution of the images of those negatively stained samples extends to only 50 Å. Further, it remains unclear whether this conformation also exists in solution.

In the present study we have determined the relative orientation of the two lobes of bovine annexin VI in the crystal by molecular replacement using x-ray diffraction data to 3.0 Å resolution. The two lobes of annexin VI are perpendicular to each other, suggesting that a major change in conformation must occur when the molecule binds to a lipid monolayer.

2. Materials and methods

2.1. Preparation

Annexin VI was isolated from bovine liver. An initial post-microsomal supernatant was prepared from fresh tissue as described by Zaks and Creutz [8] and calcium-dependent, lipid-binding proteins, including annexin VI, were extracted from this supernatant by binding to brain lipid vesicles [9]. The lipid-binding proteins were released from

* Corresponding author. Fax: +1 (804) 9825626; e-mail: rhk5i@virginia.edu.

PII S0167-4889(96)00100-0

Table 1
Data reduction

	4.0 Å set	3.5 Å set	3.0 Å set
x'tal size (mm)	0.13 × 0.13 × 0.40	0.17 × 0.17 × 0.50	0.17 × 0.17 × 0.50
Temperature (°C)	20	−173	−173
Unit cell (Å)	68.6 × 68.6 × 208.2	68.1 × 68.1 × 205.2	67.4 × 67.4 × 200.1
Resolution (Å)	30–3.3	30–3.0	30–2.5
$< I/\sigma(I) >$	7.0	9.1	20.7
< Redundancy >	3.7	3.8	3.8
Completeness (%)	81	100	99
R_{scale} (%)	19.4	14.7	6.6

the vesicles with 10 mM EGTA and fractionated on a Poros Q anion-exchange column. The fractions that contained annexin VI were precipitated with 70% saturated $(NH_4)_2SO_4$, redissolved in 30 mM KCl, 25 mM Hepes (pH 7.3) and applied to a Pharmacia Superose 12 gel filtration column. The purity of individual fractions was analyzed by SDS-PAGE. Fractions were 0.5 to 0.8 mg/ml in protein and were used directly, or after being concentrated about four fold in a Centricon cell, in hanging drop crystallizations or after addition of EGTA or addition of calcium.

2.2. Crystallization

Bovine annexin VI was crystallized by the hanging drop method. Two μl of reservoir were added to 10 μl of protein solution on the cover slip prior to inversion and placement over the well of a Linbro microtiter plate.

2.3. X-ray diffraction data measurement

Three sets of native data were measured over twenty months, each from larger crystals that diffracted with greater intensity to higher resolution. These are referred to as the 4.0 Å, the 3.5 Å, and the 3.0 Å sets. The improvements in molecular replacement calculations reflect the higher resolution and especially the intensity, or statistical significance, of the later sets. Data were measured using Cu K_α radiation, $\lambda = 1.54$ Å at 20°C (4.0 Å set), and twice at Brookhaven National Laboratory using synchrotron radiation $\lambda = 0.969$ and $\lambda = 1.009$ Å at −173°C, all three data sets were measured on image plate detectors. Data were reduced and scaled using DENZO and SCALEPACK [10,11].

2.4. Self rotation and molecular replacement calculations

Self rotation function calculations were performed with ALMN and molecular replacement calculations with AMORE, both in the CCP4 package [12]. Either human annexin V [1], or human annexin I [2], or bovine annexin IV [3] structures were used as probes. The most successful probes used full amino-acid side chains when the probe and bovine (where known, otherwise mouse) annexin VI sequences are (near) identical and truncated (usually) to Ala

Table 2
Molecular replacement translation searches (3.0 Å data set)

(a) *One search probe rotation orientation of search probe*

	#3	#1	
	5.3	4.8	Peak height
Search 1–4	15.6	18.2	Correlation coefficient
	53.1	52.8	*R*-factor
	6.2	5.6	
Search 5–8	18.3	17.0	
	52.4	52.7	

(b) *One search probe, one fixed probe rotation orientation of search probe*

	#3	#1
	11.1	13.8
Search 1–4	26.2	30.2
(5–8 fixed in other rotation)	49.8	48.8
	13.5	13.0
Search 5–8	30.2	27.7
(1–4 fixed in other rotation)	48.8	49.6

when not identical. The percentage identities of the three probes to the two lobes are similar:

annexin	I	IV	V
lobe 1–4	45%	54%	60%
lobe 5–8	46%	51%	49%

The three probe structures gave similar results; those from annexin IV are cited.

3. Results

3.1. Crystallization conditions

From the growth of the first microcrystals in 1991 [6] we have tried to get larger crystals that diffract to higher resolution. We have grown (near) isomorphous crystals from 5% w/v polyethylene glycol (PEG) 4000 (pH 7.2), 8% saturated $(NH_4)_2SO_4$ (pH 7.2), and 1.2 M sodium acetate (pH 6.7); reservoir concentrations. This range of crystallization conditions strengthens the inference that the perpendicular conformation seen in the crystal is also the form that exists in a range of solution conditions. Further, recombinant mouse annexin VI forms micro-crystals in sodium acetate that are very similar to those of bovine annexin VI.

Initially we obtained larger microcrystals in PEG and in $(NH_4)_2SO_4$ in the presence of EGTA; however, crystals of similar morphology also grew in the presence of added calcium. All three data sets were measured from crystals grown in 1.2 M sodium acetate. The 4.0 Å and the 3.5 Å crystals had no added calcium; the 3.0 Å crystal was grown in the presence of 6.0 mM added calcium. This implies that the change(s) in conformation associated with calcium binding are small enough to accommodate crystallization in the same unit cell.

3.2. Data analysis

The data measurements and molecular replacement calculations provide precedents for others determining crystal structures by Patterson search methods. The details of these analyses will be published elsewhere; several results are of more general interest. Characterization of the three sets is briefly summarized in Table 1. To approximation the first data set has information to nearly 4.0 Å resolution, the second to 3.5 Å, and the third beyond 3.0 Å; hence their respective names. The 3.5 Å data set and even the 4.0 Å set gave the correct translation function peaks. However, the significance of these peaks is much stronger with the 3.0 Å set; it has a higher $<I/\sigma(I)>$ and much lower R_{scale}.

3.3. Self rotation function

The three data sets give similar maps with the radius of integration over the range from 15 to 20 Å. The highest peak (from the 3.0 Å set) at $\alpha = 0°$, $\beta = 180°$, $\gamma = 80°$, is 85 relative to an origin of 100. This indicates a noncrystallographic two-fold rotation axis. There is one molecule per asymmetric unit; this two-fold relates lobe 1–4 to lobe 5–8.

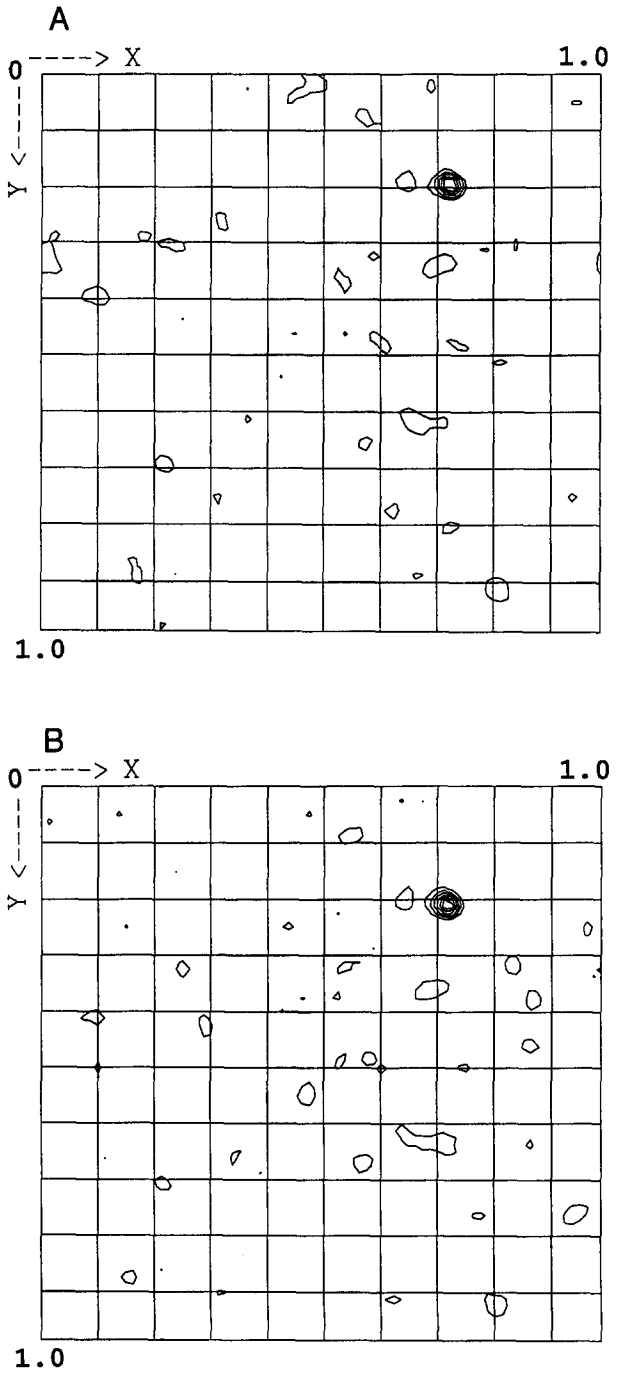

Fig. 1. Translation search with the fixed probe in one translation and rotation orientation and the search probe in the other rotation orientation. Panel a: search probe 5–8 is in #1 rotation orientation; probe 1–4 is fixed and in #3. Panel b: search probe 1–4 is in #1 rotation orientation; probe 5–8 is fixed and in #3.

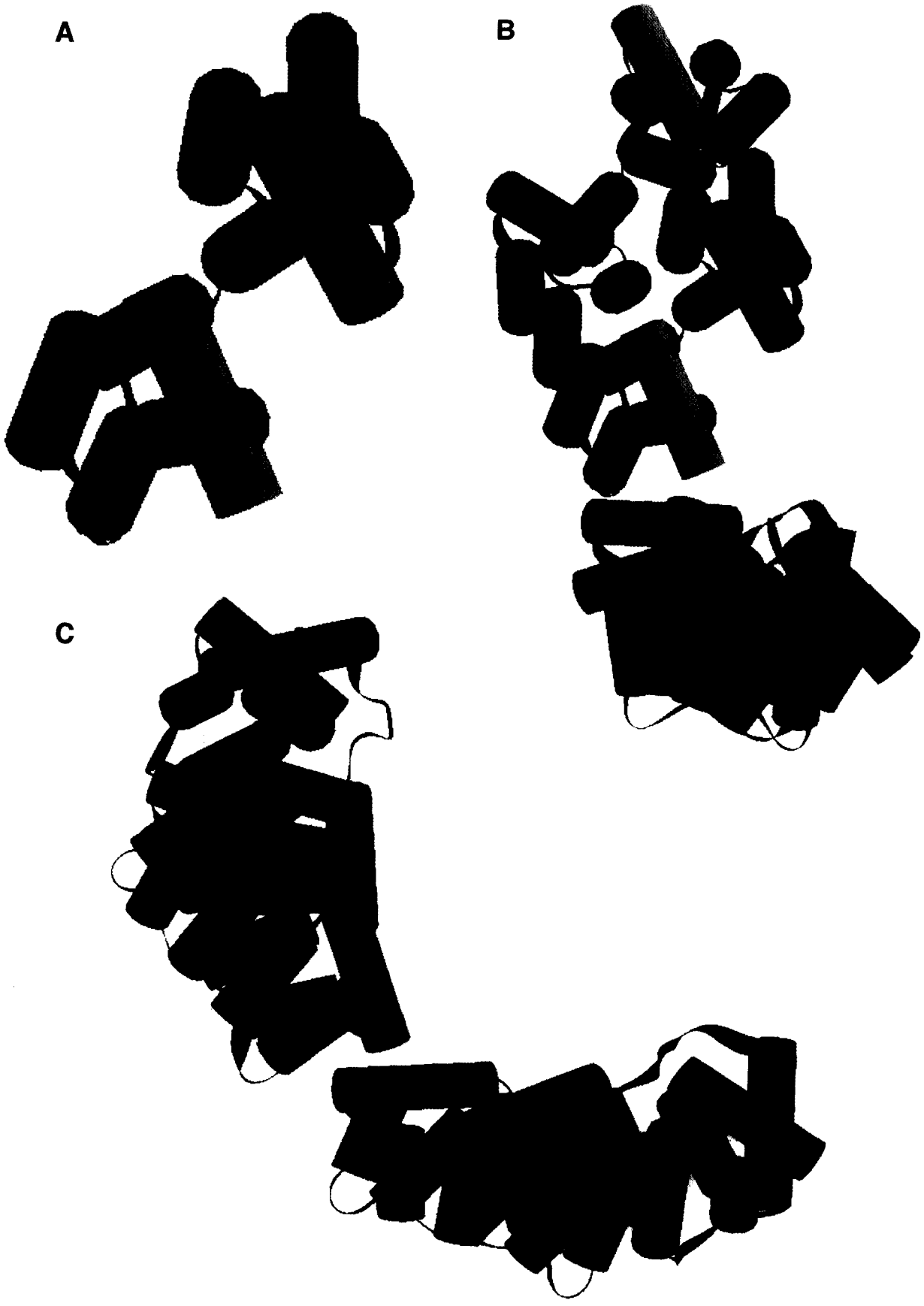
A
B
C

3.4. Molecular replacement rotation functions

Search peaks were listed in order of descending height. The highest and third highest peaks, referred to as #1 and #3, which correspond to lobe 1–4 and lobe 5–8, satisfy the constraint imposed by the self rotation function: [self] × [cross 1] = ? = [cross 2]. Several other pairs of high peaks also satisfied this condition and were evaluated. They do not yield peaks as high as the correct peaks in the subsequent translation searches.

3.5. Molecular replacement translation functions

The peak heights in Table 2a are significant. They indicate the correct space group, $P4_3$ (not $P4_1$), and confirm the rotation peaks #1 and #3. Further they suggest that probe 1–4, whose side chains had been selected to best match the amino-acid sequence of lobe 1–4, probably corresponded to rotation peak #1 and probe 5–8 to rotation peak #3. This assignment is strengthened by Table 2b. The experiment is parallel to that of Table 2a except that probe 5–8 is fixed in one orientation and translation while probe 1–4 is searched and visa versa. The assignment of probe 1–4 to peak #1 and of probe 5–8 to peak #3 is more significant than is the converse, see Fig. 1. This resolution of the pseudo symmetry of the two homologous lobes in the asymmetric unit should be confirmed with refinement.

3.6. Packing

The model from probe 1–4 in rotation orientation #1 and probe 5–8 in rotation orientation #3 packs with no interpenetration. Given lobe 1–4 at its determined position in the unit cell, one must determine which lobe 5–8 is part of the same molecule. All neighboring lobe 5–8 positions, as generated by the 4_3 screw operation and by crystallographic translations have been evaluated for steric feasibility. The relative positions of lobe 1–4 and lobe 5–8 tentatively assigned as parts of the same molecule are shown in Fig. 2. This model is being refined.

4. Discussion

The planes of the two lobes of annexin VI are rotated about 90° relative to one another in the crystal structure and supposedly in solution. Driessen et al. [7] found that the two lobes of annexin VI are coplanar when bound to a monolayer that is constrained to lie at an air, water interface. These two findings strongly imply flexibility in the linker joining lobe 1–4 and lobe 5–8. Although calcium is required for interaction with the monolayer, it appears that the perpendicular conformation of annexin VI in solution is little changed on binding calcium.

It is reasonable to anticipate intermediate conformations of annexin VI in which a less constrained membrane might be somewhat distorted.

Acknowledgements

Sandy Snyder and Kate Williams optimized the preparation of annexin VI. Initial data were measured in the laboratory of David Davies under the expert tutelage of Fred Dyda. At Brookhaven Craig Ogata kindly helped with the design and execution of measurements of the 3.5 Å and 3.0 Å data sets. We thank Robert Huber for summarizing the results of his group's determination of the crystal structure of recombinant human annexin VI as we were preparing this manuscript. This research was supported by grants from N.I.H. (GM53266 and CA40042) and from the Council for Tobacco Research (2637A).

References

[1] Huber, R., Rőmisch, J. and Pâques, E. (1990) The crystal and molecular structure of human annexin V, an anticoagulant protein that binds to calcium and membranes. EMBO J. 9, 3867–3974.
[2] Weng, S., Luecke, H., Song, I.S., Kang, D.S., Kim, S.-H. and Huber, R. (1993) Crystal structure of human annexin I at 2.5 Å resolution. Protein Sci. 2, 448–458.
[3] Sutton, R.B. and Sprang, S.R. (1996) The three dimensional structure of annexin IV, in Annexins: Molecular Structure to Cellular Function (Seaton, B.H., ed.), Landes Biosciences, Georgetown, TX.
[4] Favier-Perron, B., Lewit-Bently, A. and Russo-Marie, F. (1996) The high resolution crystal structure of human annexin III shows subtle differences with annexin V. Biochemistry 35, 1740–1744.
[5] Sűdhof, T.C., Slaughter, C.A., Leznicki, I., Barjon, P. and Reynolds, G.A. (1988) Human 67-kDa calelectrin contains a duplication of four repeats found in 35 kDa lipocortins. Proc. Natl. Acad. Sci. USA 85, 664–668.
[6] Gabriel, B.L., Taylor, K., Creutz, C.E. and Kretsinger, R.H. (1991) Microcrystals of the annexin, p68: paracrystal to crystal transition and molecular packing as determined by electron microscopy and image reconstruction. J. Struct. Biol. 107, 29–37.
[7] Driessen, H.P.C., Newman, R.H., Freemont, P.S. and Crumpton, M.J. (1992) A model of the structure of human annexin VI bound to lipid monolayers. FEBS Lett. 306, 75–79.
[8] Zaks, W.H. and Creutz, C.E. (1990) Annexin-chromaffin granule

Fig. 2. Each of the eight homologous domains of annexin VI has five helices: A (blue) runs from the inferred cytosolic surface down to the membrane surface; B (green) up to the cytosolic surface; C (yellow) across the cytosolic surface; D (orange) down to the membrane surface; and E (red) up to the cytosolic surface. Panel a: domains 5 and 6 are viewed from the cytosol. Panel b: lobe 5–8 is viewed from the cytosolic surface, looking down its local twofold axis. Lobe 1–4 is viewed edge on; its cytosolic surface is up, membrane surface to the plane of the paper. Panel c: lobe 5–8 and lobe 1–4 of panel b are rotated 90° about the vertical axis. Both lobes are seen approximately edge on.

membrane interactions: a comparative study of synexin, p32 and p67. Biochim. Biophys. Acta 1029, 149–160.
[9] Creutz, C.E., Snyder, S.L., Daigle, S.N. and Redick, J. (1996) Identification, localization and functional implications of an abundant nematode annexin. J. Cell Biol. 132, 1079–1092.
[10] Otwinowski, A. (1993) Oscillation Data Reduction Program, in Proceedings of the CCP4 Study Weekend: Data Collection and Processing (Compiled by Sawyer, L., Isaacs, N. and Bailey, S.), SERC Daresbury Laboratory, England, 1993.
[11] Minor, W. (1993) XDISPLAYF, software program, Purdue University, West Lafayette, IN.
[12] Collaborative Computational Project, #4 (1994) The CCP4 Suite: Programs for Protein Crystallography, Acta Crystallogr. A50, 157–163.